Detection of kilosecond hard lags in the new pulsating ULX candidate NGC 7456 ULX-1

Wladimiro Leone — wladimiro.leone@inaf.it
Department of Physics, University of Cagliari, Cagliari, Italy — ORCID: 0000-0002-4773-3370

F. Pintore, C. Pinto, N. O. Pinciroli Vago, A. Sanna, A. Wolter, T. Di Salvo, R. Iaria, A. D'Aì, R. Soria, P. Esposito, F. Barra, E. Ambrosi, S. Caserta, C. Salvaggio, R. Salvaterra, G. L. Israel, A. Anitra, S. Banerjee, M. Marelli, G. Rodriguez-Castillo, and L. Burderi

Introduction

Ultraluminous X-ray sources (ULXs) are off-nuclear compact accretors with $L_x > 10^{39}$ erg s^{-1} . The discovery of pulsating ULXs has demonstrated that at least a fraction of these systems host **neutron stars accreting at highly super-Eddington rates**, although the nature of the compact object remains uncertain in many sources.

Their X-ray spectra are commonly interpreted in terms of a **cool outer disk / wind photosphere**, a hotter inner accretion-flow component, and reprocessing in powerful optically thick outflows. Such winds are also thought to shape the observed timing properties.

Several ULXs show **soft X-ray lags**, usually interpreted as reverberation of hard photons in the wind. Conversely, **hard lags**, where the hard emission responds after the soft emission, are much rarer and may instead trace the inward propagation of accretion-rate fluctuations through the flow. Before this work, hard lags had been reported in only a few ULXs.

NGC 7456 ULX-1 is a particularly interesting source: it is located at distance of ~15.7 Mpc, reaches luminosities above 5×10^{39} erg s^{-1}, and exhibits extreme short-term variability (minutes to hours), and shows spectral signatures consistent with powerful super-Eddington winds.

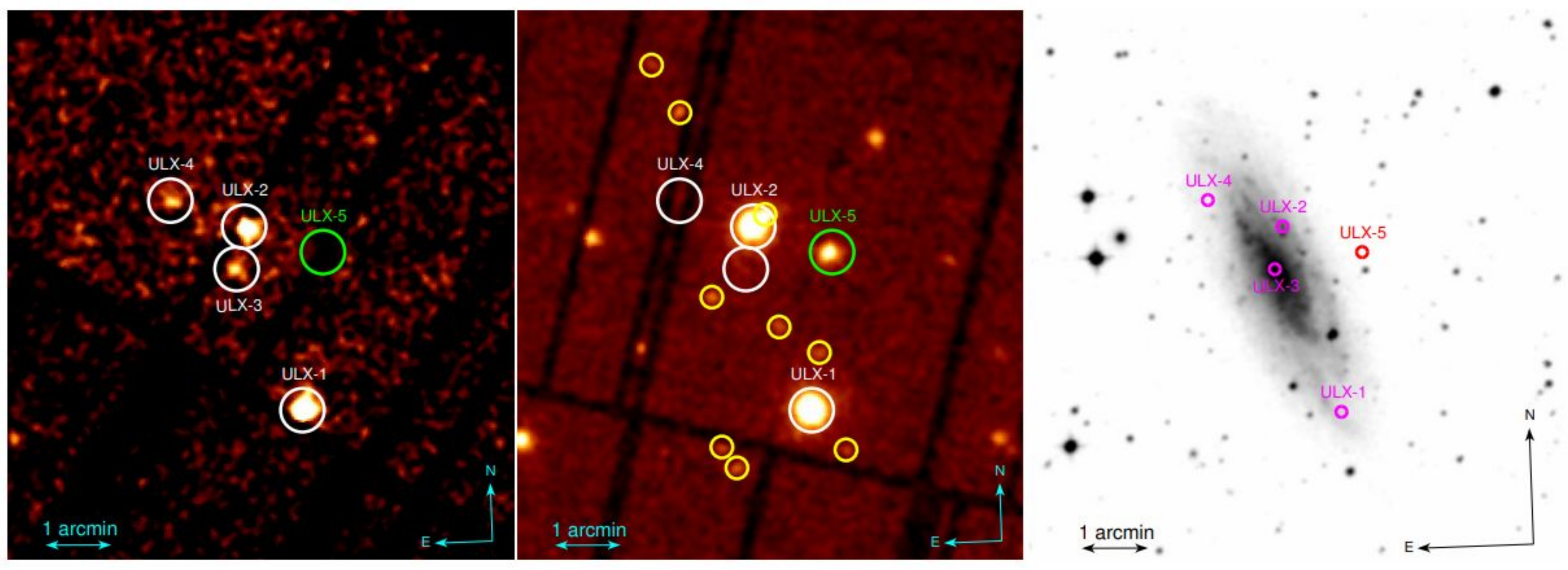

Figure 1: NGC 7456 hosts a rich ULX population, with ULX-1 among its brightest persistent X-ray sources.

Timing Analysis

Time-lag search:

We compared the **soft (0.3–1 keV)** and **hard (1–10 keV)** X-ray emission using the adaptive-binning **Cross-Correlation Function method developed in Leone et al. (2025)**, specifically optimized for the Poissonian low-count regime. These techniques offer a **crucial advantage in the low-count regime**, overcoming the limitations imposed by fixed-bin-size methods. Light curves were constructed using a fixed number of **100 photons per bin**. Lag uncertainties were derived through **Modified Double Pool (MDP) Monte Carlo simulations**.

Total hard lags:

The total lag measured over the full duration of XMM2[1] and XMM3[2] observations are:

$$\tau_{\rm tot,XMM2} = 1230 \pm 460 \text{ s}$$

$$\tau_{\rm tot,XMM3} = 1010 \pm 500 \text{ s}$$

In Fig. 2, these values are shown by the **red horizontal lines**, while the **red shaded regions represent the corresponding 1σ uncertainties** derived from the MDP Monte Carlo analysis of the full observations. In both cases, the positive lag indicates that the **soft emission leads the hard emission**, i.e. a hard lag.

Time-resolved hard lags:

To investigate the temporal evolution of the delay, we divided each observation into consecutive **10 ks intervals**, chosen as the shortest timescale providing reliable lag measurements while preserving adequate temporal resolution. The most significant hard lags are detected in the intervals showing the strongest short-term variability:

$$\tau_{\rm XMM2,1} = 1987 \pm 334 \text{ s} \qquad (0-10 \text{ ks}, \sim 5.9\sigma)$$

$$\tau_{\rm XMM3,7} = 982 \pm 345 \text{ s} \qquad (60-70 \text{ ks}, \sim 2.8\sigma)$$

These intervals coincide with pronounced variations in the **local count-rate derivative ΔI/Δt**.

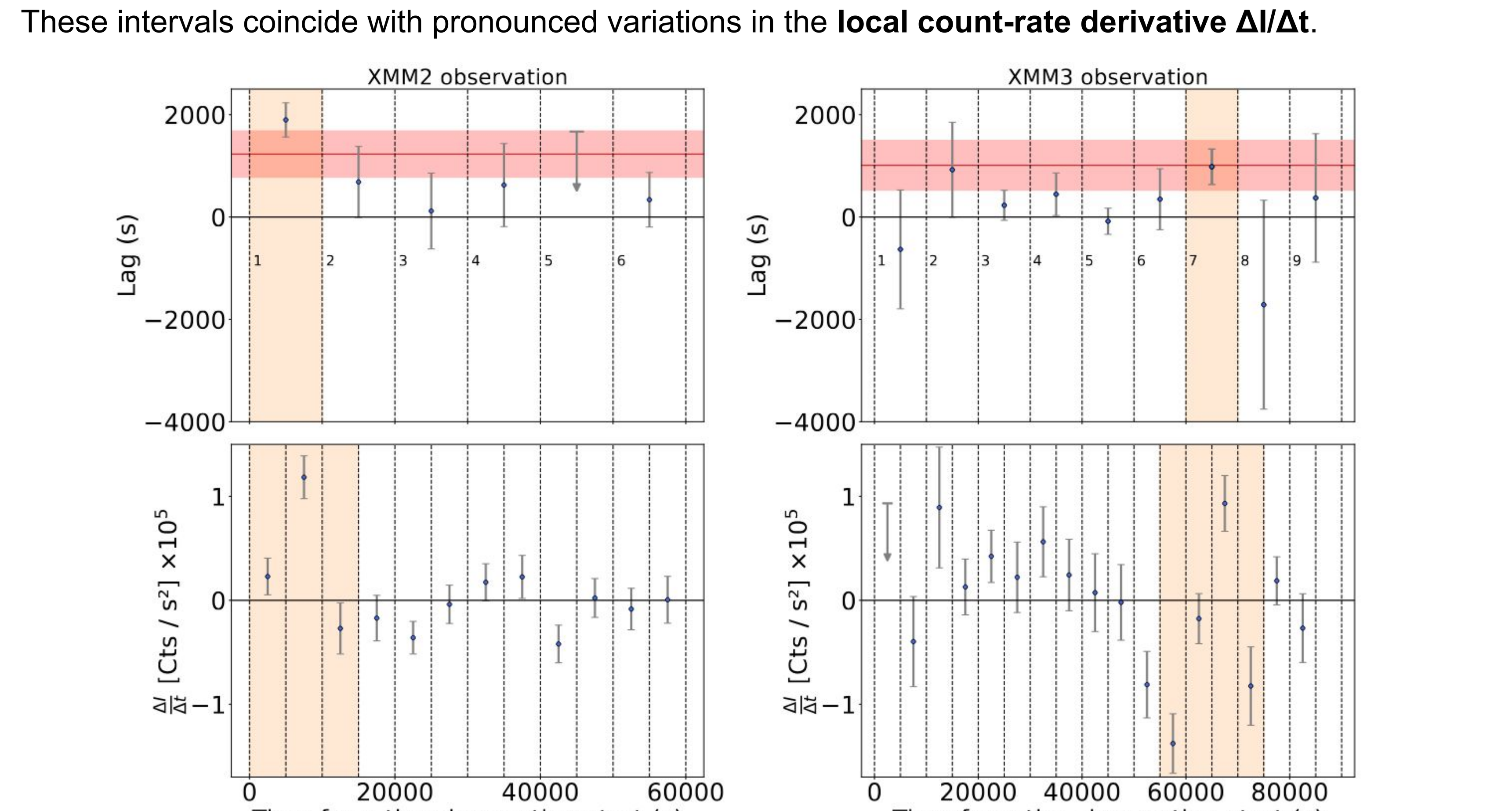

Figure 2. Time-resolved lag analysis of the two deepest XMM-Newton observations of NGC 7456 ULX-1: The upper panels show the **hard-versus-soft X-ray lag** measured in consecutive 10 ks intervals; positive values indicate that the soft band (0.3–1 keV) leads the hard band (1–10 keV), i.e. a hard lag. The **red horizontal lines** mark the total lag measured over the full observation, while the **red shaded regions** represent the corresponding 1σ uncertainties from the MDP Monte Carlo analysis. The lower panels show the **temporal evolution of the local count-rate derivative**, ΔI/Δt, evaluated in 5 ks intervals.

1. **XMM2** corresponds to the 2018 **XMM-Newton EPIC-pn+MOS** observation of NGC 7456 ULX-1, with a net exposure of **63 ks**.
2. **XMM3** corresponds to the 2023 **XMM-Newton EPIC-pn+MOS** observation, with a net exposure of **94 ks**.

Energy-resolved lags & Spectral Analysis

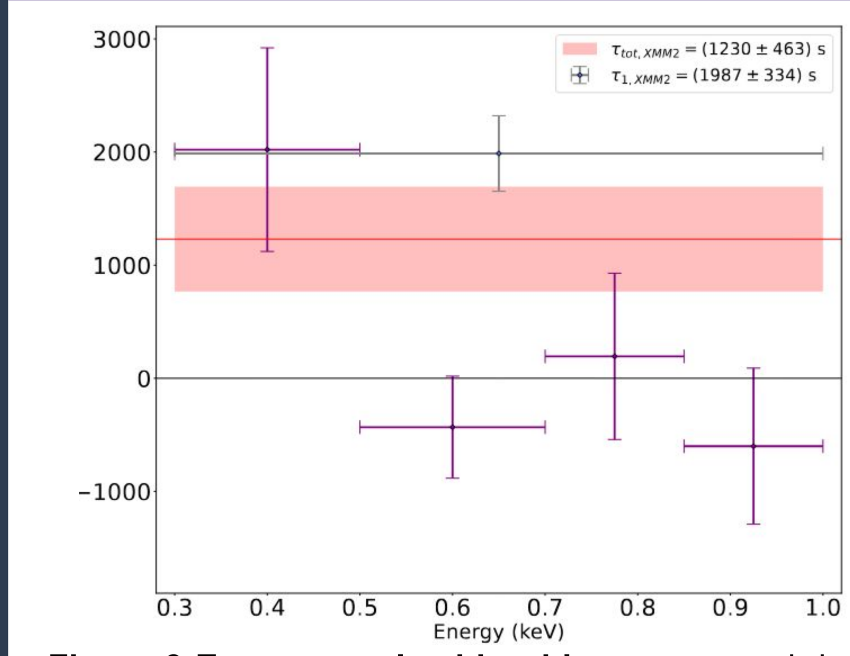

As shown in **Fig. 3**, the **energy-resolved analysis** indicates that the hard lag is primarily driven by the **lowest-energy soft X-ray photons**. In **XMM2**, the significant delay is measured between the **1–10 keV** band and the **0.3–0.5 keV** band,

$$\tau_{\rm XMM2,1}[0.3-0.5\text{ keV}] = 2225 \pm 796 \text{ s},$$

while in **XMM3** it is measured with respect to the **0.3–0.65 keV** band:

$$\tau_{\rm XMM3,7}[0.3-0.65\text{ keV}] = 1502 \pm 658 \text{ s}.$$

The slightly different soft-energy ranges adopted for **XMM2** and **XMM3** reflect the **different photon statistics** of the two observations.

Figure 3 Energy-resolved hard lags measured during the intervals showing the **strongest correlation signal**: **XMM2,1**. The **red bands** indicate the **total lag measured over the full observation**, while the **gray point** mark the lag measured in the selected **10 ks intervals**. Error bars correspond to **1σ uncertainties**.

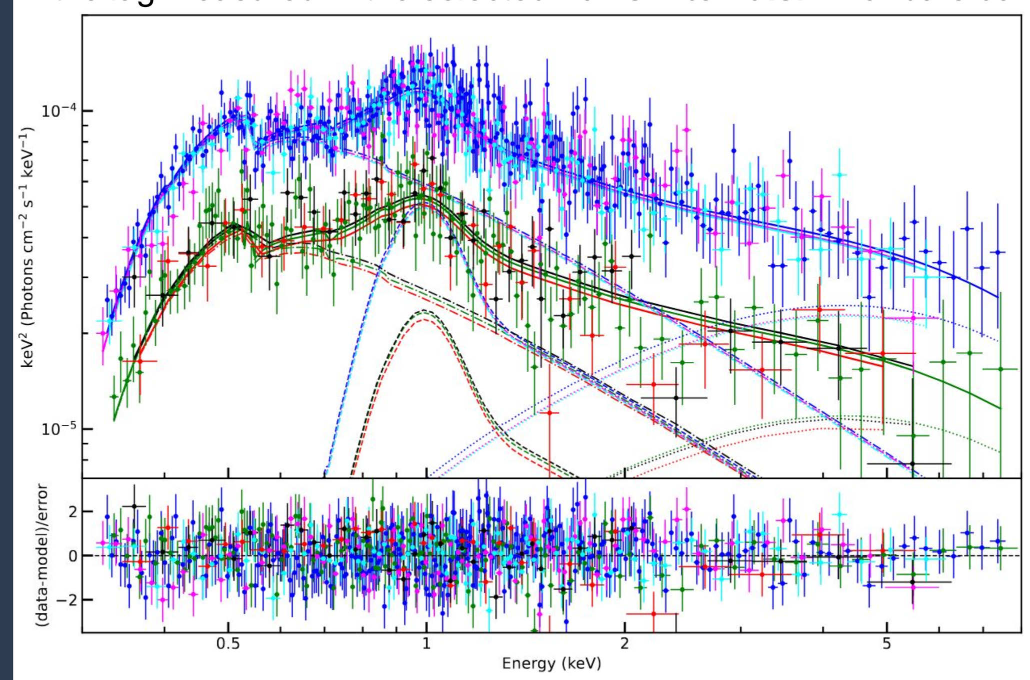

Figure 4: XMM-Newton EPIC-pn & MOS spectra for **XMM2 (2018; black, red, green)** and **XMM3 (2023; blue, cyan, purple)**. Solid/dashed curves show the best-fitting. The lower panel shows the **data-to-model residuals**.

Table 1: Best-fit spectral parameters for the joint XMM2–XMM3 spectral modelling with **TBABS×THCOMP×(GAUSS+BBODYRAD+DISKBB).** Uncertainties are reported at the **90% confidence level**.

Obs.	N_H [10^{20} cm^{-2}]	kT$_e$ [keV]	Γ^*_τ	kT$_{\rm bbrad}$ [keV]	$N_{\rm bbrad}$	kT$_{\rm diskbb}$ [keV]	$N_{\rm diskbb}$ [10^{-4}]	E$_{\rm line}$ [keV]	$\sigma_{\rm line}$ [keV]	$N_{\rm line}$ [10^{-5}]	Flux** [10^{-13} erg cm^{-2} s^{-1}]	L_X^{***} [10^{39} erg s^{-1}]	χ^2_ν – dof
XMM2	$9.3^{+4.5}_{-4.6}$	$\gtrsim 3$	$3.55^{+0.52}_{-0.74}$	$0.087^{+0.033}_{-0.036}$	297^{+2667}_{-166}	$2.06^{+4.5}_{-0.79}$	$0.95^{+6.7}_{-0.89}$	$0.918^{+0.043}_{-0.052}$	$0.109^{+0.055}_{-0.040}$	$1.77^{+0.74}_{-0.30}$	1.5 ± 0.03	4.3 ± 0.1	0.974-712
XMM3	$9.9^{+3.7}_{-3.5}$			$0.088^{+0.018}_{-0.018}$	574^{+1123}_{-388}	$1.20^{+0.92}_{-0.18}$	20^{+29}_{-18}	$0.942^{+0.026}_{-0.034}$	$0.121^{+0.041}_{-0.046}$	$3.41^{+0.83}_{-0.62}$	3.3 ± 0.03	9.4 ± 0.1	

Discussion and Conclusion

The detection of a two ~ 10^3 s **hard X-ray lags** in both XMM2 and XMM3 (**Fig. 2**) points to a recurrent property of NGC 7456 ULX-1 rather than to a single isolated variability episode. The most significant delays occur during phases of enhanced short-term variability, while the energy-resolved analysis (**Fig. 3**) shows that the lag is primarily driven by the **lowest-energy soft X-ray photons**.

The spectral decomposition (**Fig. 4; Table 1**) provides a natural physical framework for this behaviour: a **cool, extended outer region** (kT$_{\rm BB}$~0.1 keV, R$_{\rm BB}$~4×10^9 cm) coexists with a **hotter, compact inner flow** (kT$_{\rm disk}$~2 keV, R$_{\rm disk}$~16 km), whose emission is largely reprocessed in a warm, optically thick Comptonizing medium. We therefore interpret the lag through the geometry proposed in **Fig. 5**: accretion-rate fluctuations first modulate the outer soft-emitting region and then propagate inward on a viscous timescale. Hard photons produced closer to the compact object subsequently undergo additional multiple scatterings before escaping, introducing an extra diffusion delay:

$$\tau_{\rm hard} \simeq t_{\rm visc} + t_{\rm sc}$$

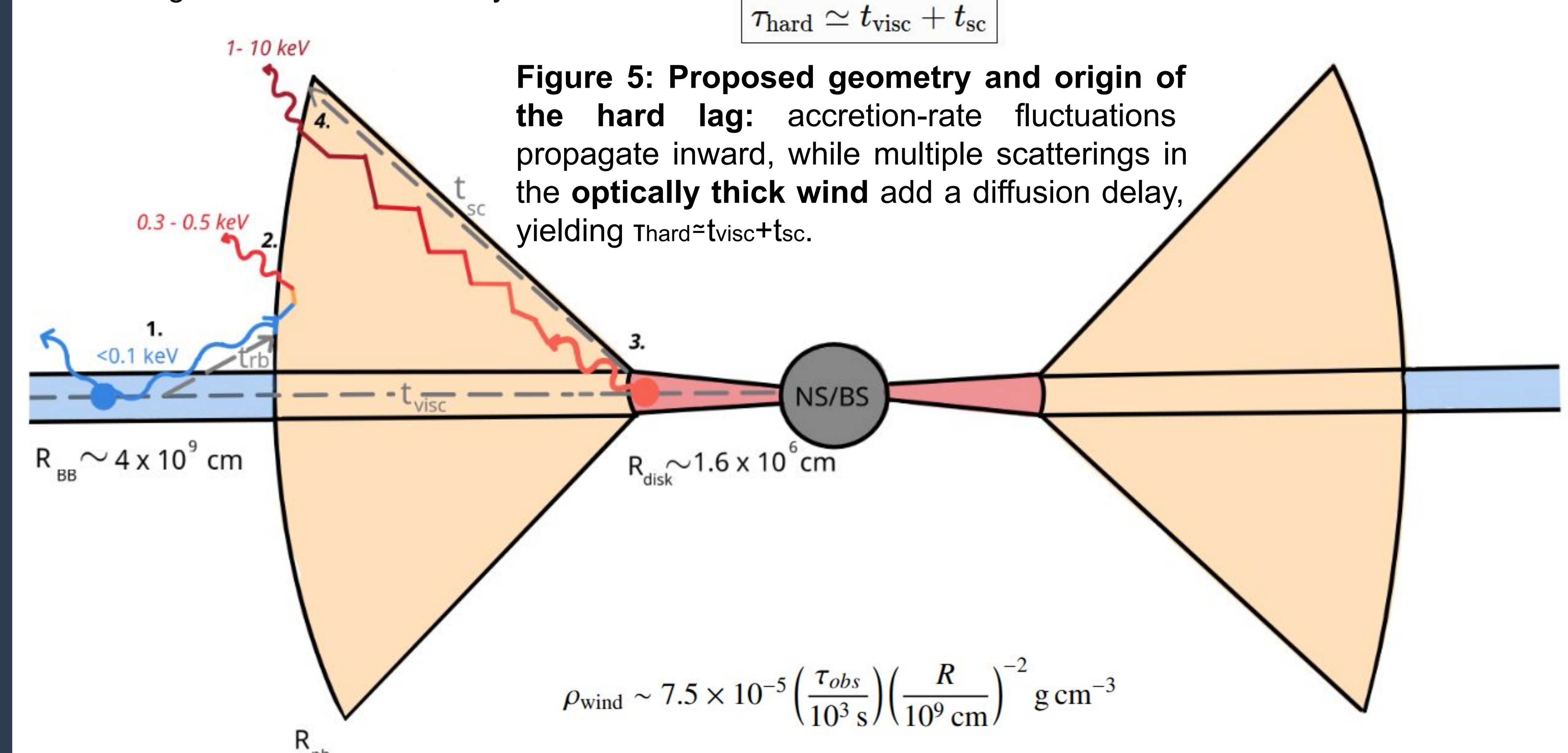

Figure 5: Proposed geometry and origin of the hard lag: accretion-rate fluctuations propagate inward, while multiple scatterings in the **optically thick wind** add a diffusion delay, yielding $\tau_{\rm hard} = t_{\rm visc} + t_{\rm sc}$.

$$\rho_{\rm wind} \sim 7.5 \times 10^{-5} \left(\frac{\tau_{obs}}{10^3 \text{ s}}\right)\left(\frac{R}{10^9 \text{ cm}}\right)^{-2} \text{g cm}^{-3}$$

This picture simultaneously explains the **sign, magnitude and energy dependence of the observed lag** and disfavors a simple reverberation scenario, which would instead produce a soft lag. If photon diffusion provides a substantial contribution to the delay, the observed ~10^3 s lag implies an effective local wind density of order **$\rho_{\rm wind}$~7.5×10^{-5} g cm^{-3}** for a characteristic scale R~10^9 cm, consistent with a dense super-Eddington outflow.

Finally, the small characteristic inner radius inferred from the spectral fit **disfavours an intermediate-mass black hole**. Together with the pulsating ULX-candidate classification and the tentative ~4.4 s periodicity, the overall spectral–timing picture is **suggestive of a neutron-star accretor**, although a stellar-mass black hole cannot yet be excluded.

Take-home message

Kilosecond hard lags offer a new window into the geometry and physics of super-Eddington accretion flows, tracing both variability propagation and radiative diffusion through optically thick winds.

Acknowledgements

I warmly thank **all my co-authors and collaborators** for their invaluable contribution to this work. This research was carried out within the **SMART-TIME postdoctoral project at the University of Cagliari**, funded through **FdS 2025**.